Wireless Networks (2023) 29:2235–2250
https://doi.org/10.1007/s11276-023-03295-8

ORIGINAL PAPER

A stochastic geometric programming approach for power allocation in wireless networks

Pablo Adasme[1] · Abdel Lisser[2]

Accepted: 20 February 2023 / Published online: 14 March 2023

Abstract
In this paper, we consider the power allocation problem for 5 G wireless networks using massive multiple input multiple output technologies. Two non-linear optimization models are considered to maximize the worst user signal-to-interference noise ratio and the total capacity of the network subject to power constraints. In particular, we transform the first one into a geometric programming (GP) problem. Whereas the second one leads to a signomial programming formulation. The main contributions of the paper are first to propose novel formulations for power allocation in wireless networks while using stochastic, geometric, and signomial programming frameworks altogether. We derive stochastic formulations for each GP model to deal with the uncertainty of wireless channels. Secondly, since solving optimally the stochastic models represents a challenging task, we obtain tight bounds using approximation solution methods. In particular, the piece-wise linear programming and the sequential approximation methods allow us to obtain tight intervals for the objective function values of the stochastic models. Notice that these intervals contain the optimal solutions. In particular, we propose an approximated GP model that allows obtaining lower bounds for the signomial problem. This is achieved by using the arithmetic–geometric mean inequality. Finally, we compare the deterministic and stochastic models and prove the robustness of the stochastic models. Notice that we solve all the instances and obtain near-optimal solutions for most of them.

Keywords Geometric and signomial programming · Sequential and piece-wise linear approximations · Wireless networks · Power allocation

1 Introduction

The fifth-generation (5G) of wireless communications brought increased attention from both academia and industry communities as it offers the potential development of unprecedented future network applications. It is expected that these networks will impact the operation of many industries and society. Example applications include mobile health, autonomous vehicles, smart cities and homes, manufacturing and entertainment, education, smart grid, data analytics, and networks to be developed under the Internet of Things (IoT) paradigm, just to name a few [1–7]. Notice that 5 G technology, as a revolutionary approach, is envisioned to eliminate access bounds to wireless networks, limitations of bandwidth capacity and latency on connectivity [7]. Unfortunately, current network infrastructures cannot be adapted straightforwardly to 5 G technology. Thus, it is mandatorily required to update previous ones. These new updates will play a critical role since novel components of 5 G networks will handle the huge increased data usage, coverage, security, and with low latency. In this paper, we consider the problem of optimal power allocation on these networks by using Massive Multiple Input Multiple Output (MaMIMO) technologies. Notice that MaMIMO appears as an extension of a traditional MIMO system. The main advantage of MaMIMO is that we can use a significantly larger number of antennas than in a classical MIMO system. It has been shown that MaMIMO allows one to achieve better performance in

✉ Pablo Adasme
pablo.adasme@usach.cl

Abdel Lisser
abdel.lisser@centralesupelec.fr

[1] Department of Electrical Engineering, Universidad de Santiago de Chile, Avenida Victor Jara 3519, Santiago 9160000, Chile

[2] Laboratoire de Signaux & Systemes L2S, Centrale Supélec Bat. Breguet A 4.22 3, rue Joliot Curie, 91190 Gif-sur-Yvette, France

terms of signal paths, link reliability, coverage, and security. As such, it emerges as a serious candidate for future 5 G based-networks.

Our main contributions in this paper can be enumerated as follows. First, we propose novel formulations for power allocation in wireless networks while using stochastic, geometric, and signomial programming frameworks altogether. Secondly, since solving optimally the stochastic models represents a challenging task, we obtain tight bounds (intervals) using approximation solution methods. In particular, the piece-wise linear programming and the sequential approximation methods allow us to obtain tight intervals for the objective function values of the stochastic models. Notice that these intervals contain the optimal solutions. Next, we propose an approximated GP model to obtain lower bounds for the signomial model. For this purpose, we use the arithmetic–geometric mean inequality. Finally, we compare the deterministic and stochastic models and prove the robustness of the stochastic models. Notice that we solve all the instances and obtain near-optimal solutions for most of the instances. More precisely, we consider two non-linear programming optimization problems for the optimal power allocation where the aim is to maximize the worst user signal-to-interference noise ratio (SINR) and the total capacity of the network subject to power constraints. In particular, we transform the first one into equivalent geometric programming (GP) problem. Whereas the second one leads to an equivalent signomial programming (SP) formulation. Notice that a GP model is a non-convex problem. However, it can be transformed into a convex one by using standard logarithmic transformations leading to ***sum-log-exp*** convex functions. Consequently, all GPs can be solved to global optimality by using interior point algorithms in polynomial time complexity [8]. Unlike a GP problem, an SP problem cannot be transformed into an equivalent convex one. Thus it is significantly harder to solve optimally. However, in this case, we also derive an approximated GP formulation that allows obtaining lower bounds for the original SP problem. The latter is achieved by using the arithmetic–geometric mean inequality [8, 9]. Subsequently, we derive stochastic formulations for each GP model to deal with the uncertainty of wireless channels. In particular, we propose individual and joint chance constraints for each GP model. Finally, we obtain lower and upper bounds with piece-wise tangent linear and sequential convex approximation methods. We conduct substantial numerical experiments to compare all the proposed models and algorithms.

A GP model is a type of mathematical optimization problem characterized by objective and constraint functions that have a special form [8]. In general, a GP model can be written as

$$\min_{\{x\in\mathbb{R}^m_{++}\}} \sum_{i\in I_0} c_i \prod_{j=1}^{m} x_j^{d_{ij}} \tag{1}$$

$$\text{s.t.} \sum_{i\in I_k} c_i \prod_{j=1}^{m} x_j^{d_{ij}} \leq 1, \quad k \in \{1,\ldots,K\} \tag{2}$$

where the set $\{I_k, k \in \mathcal{K} = \{0,1,\ldots,K\}\}$ is the disjoint index sets of $\{1,\ldots,Q\}$. Usually, the term $c_i \prod_{j=1}^{m} x_j^{d_{ij}}$ for each $i \in I_k$ is called a monomial function where each term c_i for all $i \in I_k$ must be a nonnegative real number. If at least one of them is negative, then the problem (1)-(2) is no longer a GP model, but an SP problem. The exponent parameters d_{ij} for all $i \in I_k$, $k \in \mathcal{K}$ and $j \in \mathcal{M} = \{1,\ldots,m\}$ can be real numbers. Finally, each variable x_j for $j \in \mathcal{M}$ must be strictly positive. Hereafter, we denote by R^m_{++} the set of positive real numbers of dimension m. A sum of monomials is called a posynomial function. Constraints where a monomial is strictly equal to one, are also allowed in a GP model. However, constraints involving a posynomial function strictly equal to one also lead to a non-GP problem. We will see that the arising power allocation problems considered in this paper can be written as equivalent GP or SP problems. As far as we know, individual and joint chance constraints for GP and SP problems have not been investigated in the literature for power allocation in wireless networks. Individual and joint chance constraints for the constraints in (2) can be formulated respectively as [11]

$$P_\xi\left\{\sum_{i\in I_k} c_i(\xi) \prod_{j=1}^{m} x_j^{d_{ij}} \leq 1\right\} \geq 1-\alpha, \quad k \in \{1,\ldots,K\} \tag{3}$$

and

$$P_\xi\left\{\sum_{i\in I_k} c_i(\xi) \prod_{j=1}^{m} x_j^{d_{ij}} \leq 1, \quad k \in \{1,\ldots,K\}\right\} \geq 1-\alpha \tag{4}$$

where we assume that each input parameter $(c_i(\xi))$ for all $i \in I_k$, $k \in \mathcal{K}$ behaves as a random variable which is distributed according to a certain probability distribution function. Notice that each chance constraint (3), for each $k \in \mathcal{K}$, ensures that at least $(1-\alpha)$ percentage of the uncertain constraints must be satisfied separately where α is an input parameter chosen arbitrarily from the interval [0; 0.5). Whereas the joint chance constraint (4) ensures that $(1-\alpha)$ percentage of the constraints must be satisfied according to a joint probability distribution function.

This paper is organized as follows. In Sect. 2, we present and discuss some related works which are closer to our power allocation problem. We also discuss a few relevant works related to probabilistic individual and joint chance constraints when applied to GP problems. Next, in Sect. 3, we present two non-linear optimization problems for power

allocation in 5 G wireless networks and explain how they can be transformed into equivalent GP models. Subsequently, we propose individual and joint chance constraints for each GP model and derive its equivalent deterministic formulation. Next, in Sect. 4, we present and explain the sequential approximation methods used to solve the GP models involving joint probabilistic constraints and also for solving the approximated GP models that allow computing lower bounds for the SP problem. In this section, we also present GP models using tangent piece-wise linear functions that we use to calculate lower and upper bounds for the two non-linear optimization problems. Subsequently, in Sect. 5, we conduct substantial numerical experiments and compare all the proposed models and algorithms. Finally, Sect. 6 concludes the paper.

2 Related work

Interference is a major problem in wireless networks affecting the broadcast nature of radio transmission channels. It affects data rate metrics including user signal-to-interference noise ratio as well as the maximum achievable capacity of the networks. In particular, in communication systems where users transmit in frequency bands that are non-orthogonal, it is significantly harder to deal with the interference problem. A common strategy that allows minimizing it consists of handling efficiently the amount of power to be assigned to different users. Unfortunately, several service metrics related to the interference are non-linear functions of SINR which is a non-linear and non-convex function of power. As a consequence, the arising power control optimization problems are difficult to solve optimally since they belong to the complexity class of NP-hard problems. However, some of these problems can be transformed into GP problems, and hence they can be convexified.

Some recently published papers dealing with power allocation problems in wireless networks where the geometric programming approach is utilized can be consulted for instance in [10, 12–17]. More general works can be found in references [18–23]. For the sake of brevity, we describe a few of them where the GP approach was taken into account for power allocation problems in wireless networks. In [10], the authors consider a resource allocation problem which is formulated as a non-convex problem that allows connecting a set of users to a cloud radio access network structure. To solve the problem, the authors propose an iterative algorithm that requires applying different transformations and convexification techniques and solving a sequence of GP problems with a sequential convex approximation method. By simulation results, they show that their proposed algorithm allows for increasing the total throughput of the network. Similarly in [12], the authors propose a novel framework for 5 G and beyond (5 G+) heterogeneous wireless networks which require the access of a technology referred to in the literature as power domain non-orthogonal multiple access (PD-NOMA). The main goal of their work is to maximize the total network profit under some practical technological network constraints in addition to power maximum limits, and isolation of the virtualized wireless network. They formulate the problem as a mixed integer non-linear optimization problem. To solve the model, they propose a practical approach with reduced computational complexity that consists of solving an alternating method where the optimization problem is broken down into three sub-problems. The latter is achieved by using the sequential convex approximation method, the GP approach, and a mesh adaptive direct search method. Their numerical experiments reveal that the proposed approach can improve the overall network profit. Also, in [15] the authors consider a resource allocation problem for uplink non-orthogonal multiple access networks for health and public safety applications. The authors apply a chance-constrained robust optimization approach leading to a joint resource allocation problem that allows minimizing user transmit power subject to rate and outage constraints. Since their resulting non-linear problem is non-convex, they apply variable relaxation and complementary geometric programming approaches and develop a two-step iterative algorithm based on successive convex approximations. By simulation results, the authors demonstrate that their proposed algorithm outperforms the traditional orthogonal multiple access transmission schemes in terms of user transmit power and overall system density using fewer sub-carriers. Finally, we mention the work proposed by [24] where the authors present several power allocation models that can be equivalently written as GP problems. Their examples include maximizing the total system throughput or the worst user throughput, subject to the quality of service constraints, delay constraints on data rates, and outage probabilities.

As can be observed from the literature, several relevant problems related to future wireless networks utilized the GP approach to solve specialized resource allocation problems. However, we notice that there have been no attempts yet to include stochastic individual or joint chance constraints in these types of problems to handle efficiently the uncertainty of the input parameters. The chance-constrained approach allows imposing a probability of occurrence for some or all of the constraints of a mathematical programming problem. This means that some of the constraints will be satisfied, at least for a given percentage of the occurrences of each random variable. Probabilistic constraints can be considered either separately or jointly. Notice that the stochastic programming framework is a

relevant approach in the literature and is frequently considered in optimization problems. It allows for obtaining optimal solutions while taking into account the uncertainty of the input parameters of a mathematical programming problem [25–33]. In particular, the authors in [34, 35] show that the probabilistic constraint (3) can be equivalently written employing two deterministic constraints involving posynomials and slack variables. To the best of our knowledge, there are only a few works in the literature including stochastic GP problems subject to joint probabilistic constraints. In [11], the authors impose joint probabilistic constraints on a generic GP problem and assume that the input stochastic parameters are normally distributed and independent of each other. They approximate the problem by using piece-wise linear functions which allow transforming the resulting problem into an equivalent convex geometric program. They also prove that their approximation model allows obtaining lower bounds for the original problem. Finally, they design a sequential convex optimization algorithm that allows obtaining upper bounds for the original problem too. Similarly, the authors in [36] discuss joint rectangular probabilistic constrained GPs. For this purpose, they assume that the input random parameters are elliptically distributed and pairwise independent. The authors obtain a non-convex reformulation of the joint rectangular chance-constrained problem and propose convex approximations using variable transformation and piece-wise linear functions. Finally, they provide a theoretical bound for the number of segments in the worst-case scenario and show by numerical experiments that their approximations are asymptotically tight.

A few other recently published works dealing with resource allocation of power in wireless networks where the approaches proposed in this paper could be applied as part of future research can be briefly described as follows. In [43], the authors propose a dynamic optimization model to maximize the total uplink and/or downlink energy efficiency while satisfying quality of service constraints using as a viable solution the Mobile Edge Computing (MEC) paradigm to satisfy the growing demand for broadband for the next generation heterogeneous systems. The authors divide the optimization problem into two separate subproblems, a computational carrier scheduling one, and a resource allocation problem. In particular, they propose a sub-gradient method for the computational resource allocation and a successive convex approximation together with a dual decomposition method. Their simulation results show considerable improvements for various traffic models guaranteeing fairness requirements. It also improved the total throughput for mobile computing services. Similarly, in [44] the authors present a deep learning-based mobility robustness optimization solution that learns the required parameter values for the mobility pattern for self-organizing networks. Their simulation experiments show that the function of mobility robustness optimization not only learns to optimize its performance but also it learns how to distribute the excess load of the network. Finally, they prove that the solution minimizes the number of unsatisfied users guaranteeing a more balanced network. Finally, in reference [45], the authors consider a dynamic optimization model to minimize the total energy consumption of fifth-generation (5 G) heterogeneous networks while providing the required coverage and capacity. This is achieved by optimizing carrier allocation and power utilization. They do also propose a multi-hop back-hauling strategy to effectively use the existing infrastructure of small-cell networks for simultaneous transmissions. Their numerical results demonstrated considerable power savings for different traffic models. They further show that energy efficiency and system data rates can be significantly improved.

3 Mathematical formulations

In this section, first, we present the two non-linear optimization problems. Then, for each one of them, we derive equivalent GP formulations. In particular, for the second one, we obtain an equivalent SP formulation. Thus, we derive an approximated GP model that allows obtaining lower bounds for it. Subsequently, we impose individual and joint chance constraints on each GP model obtained and derive for each one of them an equivalent deterministic GP formulation.

3.1 Maximizing the worst user signal to interference noise ratio

The first model we consider allows maximizing the worst user signal-to-interference noise ratio for a MaMIMO system where each receiver has perfect channel state information [37]. Hereafter, we assume that the MaMIMO network is located inside a single cell area and it is composed of a set of $\mathcal{K} = \{1, \ldots, K\}$ users and a unique base station (BS). We also assume that each user is using only one antenna to receive the data from the BS which is equipped with a predefined number of antennas T. We formulate the optimization problem as

$$(M_1): \max_{\{p \in \mathbb{R}^K_{++}\}} \min_{\{i \in \mathcal{K}\}} \left\{ \frac{p_i \mid g_i^H g_i \mid^2}{\sum_{j \in \mathcal{K}, (j \neq i)} p_j \mid g_i^H g_j \mid^2 + \mid \sigma_i \mid^2} \right\} \tag{5}$$

$$\text{s.t. } P_{min} \leq p_i \leq P_{max}, \quad \forall i \in \mathcal{K} \tag{6}$$

where $p = (p_i)$ denotes the amount of power to be assigned for each user $i \in \mathcal{K}$. The input parameters $g_i \in \mathbf{C}^{T\times 1}$, $g_i^H \in \mathbf{C}^{1\times T}$ and σ_i denotes the beam domain channel vector associated to user $i \in \mathcal{K}$, its Hermitian transpose and Additive White Gaussian Noise (AWGN), respectively. The AWGN is assumed to behave according to an independent complex Gaussian distribution function with zero mean and unit variance ($\sigma_i \sim \mathcal{CN}(0,1)$). Finally, we assume that each component of each vector g_i, $i \in \mathcal{K}$ is a complex number generated according to a quasi-static independent and identically distributed Rayleigh fading channel. Notice that from the solution of model (M_1), a power allocation mechanism can be designed by simply using the power allocation vector obtained from the model. Similarly, the worst user SINR can be easily obtained from the value of the objective function since we use a unique variable for all users in $\mathcal{K}$. This objective function value will coincide with the user or users having the maximum worst SINR.

In (M_1), the objective function (5) denotes the worst user SINR [38, 39]. Whilst the constraints (6) ensure that each power variable is greater than or equal to P_{min} and less than or equal to P_{max}. Notice that by introducing an additional variable t and defining the parameters $a_{ij} = \mid g_i^H g_j \mid^2 \mid g_i^H g_i \mid^{-2} > 0$ and $b_i = \mid \sigma_i^2 \mid\mid g_i^H g_i \mid^{-2} > 0$ for all $i,j \in \mathcal{K}$, we can write (M_1) equivalently as

$$\min_{\{(p,t)\in\mathbb{R}_{++}^{K+1}\}} t^{-1} \tag{7}$$

$$\begin{aligned} \text{s.t.} \sum_{j\in\mathcal{K},(j\neq i)} a_{ij}p_j p_i^{-1}t + b_i p_i^{-1}t \leq 1, \quad \forall i \in \mathcal{K} \\ P_{min} \leq p_i \leq P_{max}, \quad \forall i \in \mathcal{K} \end{aligned} \tag{8}$$

We note that the coefficients a_{ij} and b_i in (8) for all $i,j \in \mathcal{K}$, may not be known precisely. Thus, we suppose that each one of them is normally distributed and independent of the other, i.e., $a_{ij}(\xi) \sim \mathcal{N}(\bar{a}_{ij}, \sigma_{a_{ij}}^2)$ and $b_i(\xi) \sim \mathcal{N}(\bar{b_i}, \sigma_{b_i}^2)$. This allows replacing the deterministic constraints in (8) with the following individual chance constraints

$$\begin{aligned} \mathbb{P}_\xi \left\{ \sum_{j\in\mathcal{K},(j\neq i)} a_{ij}(\xi)p_j p_i^{-1}t + b_i(\xi)p_i^{-1}t \leq 1 \right\} \\ \geq (1-\alpha), \quad \forall i \in \mathcal{K} \end{aligned} \tag{9}$$

According to [34], the constraints (9) can be written in equivalent deterministic form as

$$\begin{aligned} \sum_{j\in\mathcal{K},(j\neq i)} \bar{a}_{ij}p_j p_i^{-1}t + \bar{b_i}p_i^{-1}t \\ + \phi^{-1}(1-\alpha)\left\{ \sqrt{\sum_{j\in\mathcal{K},(j\neq i)} \sigma_{a_{ij}}^2 p_j^2 p_i^{-2}t^2 + \sigma_{b_i}^2 p_i^{-2}t^2} \right\} \\ \leq 1, \forall i \in \mathcal{K} \end{aligned} \tag{10}$$

where $\phi^{-1}(1-\alpha)$ is the quantile of the standard normal distribution function $\mathcal{N}(0,1)$. The parameter α can take values in the interval $\alpha \in [0; 0.5)$. Notice that the constraints (10) are generalized posynomial constraints. Thus, they can be transformed into standard GP format. The latter can be achieved by introducing additional variables $\theta_i > 0$ for all $i \in \mathcal{K}$. This allows imposing an upper bound on each term inside the root square

$$\sum_{j\in\mathcal{K},(j\neq i)} \sigma_{a_{ij}}^2 p_j^2 p_i^{-2}t^2 + \sigma_{b_i}^2 p_i^{-2}t^2 \leq \theta_i^2, \quad \forall i \in \mathcal{K} \tag{11}$$

which in turn allows obtaining the equivalent set of constraints

$$\sum_{j\in\mathcal{K},(j\neq i)} \bar{a}_{ij}p_j p_i^{-1}t + \bar{b_i}p_i^{-1}t + \phi^{-1}(1-\alpha)\theta_i \leq 1, \quad \forall i \in \mathcal{K} \tag{12}$$

$$\sum_{j\in\mathcal{K},(j\neq i)} \sigma_{a_{ij}}^2 p_j^2 p_i^{-2}t^2\theta_i^{-2} + \sigma_{b_i}^2 p_i^{-2}t^2\theta_i^{-2} \leq 1, \quad \forall i \in \mathcal{K} \tag{13}$$

Notice that the constraints (12)-(13) prove that the resulting problem is a GP problem. Consequently, we can obtain the global optimal solution using individual chance constraints by solving the following GP model

$$\begin{aligned} (IM_1): \min_{\{(p,t)\in\mathbb{R}_{++}^{K+1}\}} t^{-1} \\ \text{s.t.} \sum_{j\in\mathcal{K},(j\neq i)} \bar{a}_{ij}p_j p_i^{-1}t + \bar{b_i}p_i^{-1}t + \\ \phi^{-1}(1-\alpha)\left\{ \sqrt{\sum_{j\in\mathcal{K},(j\neq i)} \sigma_{a_{ij}}^2 p_j^2 p_i^{-2}t^2 + \sigma_{b_i}^2 p_i^{-2}t^2} \right\} \leq 1, \\ \forall i \in \mathcal{K} \\ P_{min} \leq p_i \leq P_{max}, \quad \forall i \in \mathcal{K} \end{aligned}$$

Similarly, we can replace the deterministic constraints (8) by the following joint probabilistic constraints

$$\begin{aligned} \mathbb{P}_\xi \left\{ \sum_{j\in\mathcal{K},(j\neq i)} a_{ij}(\xi)p_j p_i^{-1}t + b_i(\xi)p_i^{-1}t \leq 1, \forall i \in \mathcal{K} \right\} \\ \geq (1-\alpha) \end{aligned} \tag{14}$$

As these constraints are equivalent, we have

$$\prod_{i\in\mathcal{K}} \mathbb{P}_{\xi}\left(\sum_{j\in\mathcal{K},(j\neq i)} a_{ij}(\xi)p_j p_i^{-1}t + b_i(\xi)p_i^{-1}t \leq 1\right) \geq (1-\alpha) \tag{15}$$

Next, by introducing auxiliary variables $y_i \in \mathbb{R}_{++}$ for all $i \in \mathcal{K}$, we get the following equivalent deterministic GP problem using joint chance constraints [11, 34, 35]

$$\begin{aligned}(JM_1): \min_{\{(p,t,y)\in\mathbb{R}^{2K+1}_{++}\}} \; & t^{-1} \\ \text{s.t.} \; & \sum_{j\in\mathcal{K},(j\neq i)} \bar{a}_{ij}p_j p_i^{-1}t + \bar{b}_i p_i^{-1}t + \\ & \phi^{-1}(y_i)\left\{\sqrt{\sum_{j\in\mathcal{K},(j\neq i)} \sigma^2_{a_{ij}} p_j^2 p_i^{-2}t^2 + \sigma^2_{b_i} p_i^{-2}t^2}\right\} \\ & \leq 1, \\ & \forall i \in \mathcal{K}\end{aligned} \tag{16}$$

$$\prod_{i\in\mathcal{K}} y_i \geq (1-\alpha) \tag{17}$$

$$\begin{aligned}& 0 \leq y_i \leq 1, \quad \forall i \in \mathcal{K} \\ & P_{min} \leq p_i \leq P_{max}, \quad \forall i \in \mathcal{K}\end{aligned} \tag{18}$$

Notice that the quantile function now depends on the variable y_i for all $i \in \mathcal{K}$. In the next section, we obtain lower and upper bounds for (JM_1) using tangent piece-wise linear functions as well as a sequential approximation algorithm [11]. This allows reporting an interval where the global optimal solution lies.

3.2 Maximizing the total capacity of the wireless network

The second model we consider maximizes the total capacity of the network in presence of signal-to-interference noise ratio for a MaMIMO system where each receiver has a perfect channel state information [37]. In this case, the non-linear optimization problem we consider can be stated as

$$\begin{aligned}(M_2): \max_{\{p\in\mathbb{R}^K_{++}\}} \; & \sum_{i\in\mathcal{K}} \log_2\left(1 + \frac{p_i \mid g_i^H g_i \mid^2}{\sum_{j\in\mathcal{K}} p_j \mid g_i^H g_j \mid^2 + \mid \sigma_i \mid^2}\right) \\ & (j\neq i) \\ \text{s.t.} \; & P_{min} \leq p_i \leq P_{max}, \quad \forall i \in \mathcal{K}\end{aligned} \tag{19}$$

Similarly as for (M_1), we redefine the nonnegative parameters $a_{ij} = \mid g_i^H g_j \mid^2 > 0$ and $b_i = \mid \sigma_i \mid^2 > 0$ for all $i,j \in \mathcal{K}$.

Claim 1 *(M_2) can be equivalently written as a signomial programming problem.*

Proof First, notice that

$$\begin{aligned}&\sum_{i\in\mathcal{K}} \log_2\left(1 + \frac{p_i \mid g_i^H g_i \mid^2}{\sum_{j\in\mathcal{K}} p_j \mid g_i^H g_j \mid^2 + \mid \sigma_i \mid^2}\right) \\ &\qquad (j\neq i) \\ &= \log_2\left(\prod_{i\in\mathcal{K}}\left(1 + \frac{p_i \mid g_i^H g_i \mid^2}{\sum_{j\in\mathcal{K}} p_j \mid g_i^H g_j \mid^2 + \mid \sigma_i \mid^2}\right)\right)\end{aligned}$$

Next, we introduce a lower bound variable t_i for each $i \in \mathcal{K}$ in order to obtain an optimal solution for (M_2) by solving the following equivalent problem

$$\begin{aligned}\max_{\{(p,t)\in\mathbb{R}^{2K}_{++}\}} \; & \prod_{i\in\mathcal{K}} t_i \\ \text{s.t.} \; & t_i \leq 1 + \frac{a_{ii}p_i}{\sum_{j\in\mathcal{K},(j\neq i)} a_{ij}p_j + b_i}, \quad \forall i \in \mathcal{K} \\ & P_{min} \leq p_i \leq P_{max}, \quad \forall i \in \mathcal{K}\end{aligned} \tag{20}$$

In particular, we note that the constraints (20) can be written as

$$\frac{\sum_{j\in\mathcal{K},(j\neq i)} a_{ij}p_j t_i + b_i t_i}{\sum_{j\in\mathcal{K},(j\neq i)} a_{ij}p_j + b_i + a_{ii}p_i} \leq 1, \quad \forall i \in \mathcal{K} \tag{21}$$

or as

$$\sum_{j\in\mathcal{K},(j\neq i)} a_{ij}b_i^{-1}p_j t_i + t_i - \sum_{j\in\mathcal{K}} a_{ij}b_i^{-1}p_j \leq 1 \quad \forall i \in \mathcal{K} \tag{22}$$

Notice that the left-hand side of constraint (22) has negative coefficients which show that (M_2) leads to a signomial programming problem. □

Because of Claim 1, we see that finding a global optimal solution for (M_2) is significantly harder than solving a GP problem. However, we can still approximate each posynomial function in the denominator of the constraints (21) with a monomial function to obtain a lower bound for (M_2) [8]. This can be achieved by using the arithmetic–geometric mean inequality. Thus, we have the following proposition.

Proposition 1 *For fixed and nonnegative parameter values δ_{ij} and β_i for all $i,j \in \mathcal{K}$ such that $\sum_{j\in\mathcal{K}} \delta_{ij} + \beta_i = 1$, for all $i \in \mathcal{K}$, the following GP model gives a lower bound for (M_2)*

$$Q(\delta,\beta)=\max_{\{(p,t)\in\mathbb{R}^{2K}_{++}\}}\prod_{i\in\mathcal{K}}t_i \tag{23}$$

$$\text{s.t. }\prod_{l\in\mathcal{K}}p_l^{-\delta_{il}}\left(\sum_{j\in\mathcal{K},(j\neq i)}c_{ij}p_jt_i+d_it_i\right)\leq 1,\quad \forall i\in\mathcal{K} \tag{24}$$

$$P_{min}\leq p_i\leq P_{max},\quad \forall i\in\mathcal{K}$$

where

$$c_{il}=a_{il}\prod_{j\in\mathcal{K}}\left(\frac{a_{ij}}{\delta_{ij}}\right)^{-\delta_{ij}}(b_i\beta_i^{-1})^{-\beta_i},\quad \forall i,l\in\mathcal{K},(i\neq l)$$

and

$$d_i=b_i\prod_{j\in\mathcal{K}}\left(\frac{a_{ij}}{\delta_{ij}}\right)^{-\delta_{ij}}(b_i\beta_i^{-1})^{-\beta_i},\quad \forall i\in\mathcal{K}$$

Proof Notice that by applying the arithmetic–geometric mean inequality we have that

$$\sum_{j\in\mathcal{K}}a_{ij}p_j+b_i\geq\prod_{j\in\mathcal{K}}\left(\frac{a_{ij}p_j}{\delta_{ij}}\right)^{\delta_{ij}}\left(b_i\beta_i^{-1}\right)^{\beta_i},\quad \forall i\in\mathcal{K} \tag{25}$$

for values of $\delta_{ij}\geq 0$, $\beta_i\geq 0$ for all $i,j\in\mathcal{K}$ with respect to $\sum_{j\in\mathcal{K}}\delta_{ij}+\beta_i=1$ for all $i\in\mathcal{K}$. We do also have

$$\frac{\sum_{j\in\mathcal{K},(j\neq i)}a_{ij}p_jt_i+b_it_i}{\sum_{j\in\mathcal{K}}a_{ij}p_j+b_i}\leq\frac{\sum_{j\in\mathcal{K},(j\neq i)}a_{ij}p_jt_i+b_it_i}{\prod_{j\in\mathcal{K}}\left(\frac{a_{ij}p_j}{\delta_{ij}}\right)^{\delta_{ij}}\left(b_i\beta_i^{-1}\right)^{\beta_i}} \tag{26}$$
$$\leq 1,\quad \forall i\in\mathcal{K}$$

Next, by performing simple algebraic manipulations in the latter inequalities we obtain

$$\prod_{l\in\mathcal{K}}p_l^{-\delta_{il}}\left(\sum_{j\in\mathcal{K},(j\neq i)}c_{ij}p_jt_i+d_it_i\right)\leq 1,\quad \forall i\in\mathcal{K}, \tag{27}$$

Finally, a lower bound for (M_2) can be obtained by calculating the logarithm of the objective function in (23). Thus, concluding the proof. □

Notice that the inequalities (25) have zero gaps when all the involved terms in the sum and the product are equal. Furthermore, we observe from Proposition 1 that we can adjust the parameter δ_{ij} and β_i for all $i,j\in\mathcal{K}$ to tighten the lower bound obtained with $Q(\delta,\beta)$. More precisely, we see that the optimal values for the parameters δ_{ij} and β_i for all $i,j\in\mathcal{K}$ can be obtained by solving the following optimization problem

$$Q(\delta^*,\beta^*)=\max_{\{(\delta,\beta)\in\mathbb{R}_+^{K^2+K}\}}Q(\delta,\beta) \tag{28}$$

$$\text{s.t. }\sum_{j\in\mathcal{K}}\delta_{ij}+\beta_i=1,\quad \forall i\in\mathcal{K} \tag{29}$$

Unfortunately, finding the global optimal solution of problem (28)-(29) is not trivial as it is a non-convex problem. However, in an attempt to find its global optimal solution, we can still solve the problem with an iterative algorithm referred to as the single condensation method in the literature which is essentially a sequential approximation method [24]. In general, with this method, we can obtain a locally optimal solution to the problem. However, a common strategy may consist of generating different initial solutions for model (28)-(29) to increase the chances to obtain the global optimal solution for model (M_2). In the next section, we explain how we apply this method to obtain a lower bound for (M_2).

Notice that analogously as for the model (M_1), we can assume that the input parameters c_{ij} and d_i for all $i,j\in\mathcal{K}$ in model $Q(\delta,\beta)$ are random variables normally and independently distributed, i.e., $c_{ij}(\xi)\sim\mathcal{N}(\bar{c}_{ij},\sigma^2_{c_{ij}})$ and $d_i(\xi)\sim\mathcal{N}(\bar{d}_i,\sigma^2_{d_i})$, respectively. This allows writing the following stochastic version of $Q(\delta,\beta)$ with individual chance constraints

$$\begin{aligned}(IM_2):\ &\max_{\{(p,t)\in\mathbb{R}^{2K}_{++}\}}\prod_{i\in\mathcal{K}}t_i\\ &\text{s.t. }\prod_{l\in\mathcal{K}}p_l^{-\delta_{il}}\left(\sum_{j\in\mathcal{K},(j\neq i)}\bar{c}_{ij}p_jt_i+\bar{d}_it_i\right)\\ &\quad+\phi^{-1}(1-\alpha)\left\{\sqrt{\prod_{l\in\mathcal{K}}p_l^{-2\delta_{il}}\left(\sum_{j\in\mathcal{K},(j\neq i)}\sigma^2_{c_{ij}}p_j^2t_i^2+\sigma^2_{d_i}t_i^2\right)}\right\}\\ &\quad\leq 1,\\ &\quad\forall i\in\mathcal{K}\\ &\quad P_{min}\leq p_i\leq P_{max},\quad \forall i\in\mathcal{K}\end{aligned} \tag{30}$$

Observe that model (IM_2) is a GP problem and then, it can be solved optimally. Finally, we can also arrive at the following stochastic optimization problem with joint chance constraints

$$
\begin{aligned}
(JM_2): \quad & \max_{\{(p,t,y)\in\mathbb{R}^{3K}_{++}\}} \prod_{i\in\mathcal{K}} t_i \\
\text{s.t.} \quad & \prod_{l\in\mathcal{K}} p_l^{-\delta_{il}} \left(\sum_{j\in\mathcal{K},(j\neq i)} \bar{c}_{ij} p_j t_i + \bar{d}_i t_i \right) \\
& + \phi^{-1}(y_i) \left\{ \sqrt{\prod_{l\in\mathcal{K}} p_l^{-2\delta_{il}} \left(\sum_{j\in\mathcal{K},(j\neq i)} \sigma^2_{c_{ij}} p_j^2 t_i^2 + \sigma^2_{d_i} t_i^2 \right)} \right\} \\
& \leq 1, \\
& \forall i \in \mathcal{K} \\
& \prod_{i\in\mathcal{K}} y_i \geq (1-\alpha) \\
& 0 \leq y_i \leq 1, \quad \forall i \in \mathcal{K} \\
& P_{min} \leq p_i \leq P_{max}, \quad \forall i \in \mathcal{K}
\end{aligned}
\tag{31}
$$

Similarly as for (JM_1), in the next section, we compute bounds for (JM_2) using piece-wise linearization and sequential approximation methods.

4 Piece-wise linear and sequential approximation methods

In this section, we present two GP models using a tangent piece-wise linear approximation method for computing lower and upper bounds for (JM_1) and (JM_2), respectively. Then, we present a sequential approximation algorithm to obtain upper and lower bounds for (JM_1) and (JM_2), respectively. Finally, we present a single condensed sequential approximation method used to compute lower bounds for model $Q(\delta,\beta)$ (See proposition 1). We mention that in order to solve the models (IM_2) and (JM_2), we use the best parameter values (δ^*,β^*) obtained with the single condensation method.

4.1 GP models obtained using tangent piece-wise linear functions

According to Theorem 1 in [11], we can compute lower and upper bounds for (JM_1) and (JM_2) by solving the following GP models

$$
\begin{aligned}
(JM_1)^{Lb}: \quad & \min_{\{(p,t,y)\in\mathbb{R}^{2K+1}_{++}\}} t^{-1} \\
\text{s.t.} \quad & \sum_{j\in\mathcal{K},(j\neq i)} \bar{a}_{ij} p_j p_i^{-1} t + \bar{b}_i p_i^{-1} t \\
& + \left(e^{\frac{f_s}{2}} y_i^{\frac{g_s}{2}} \right) \left\{ \sqrt{\sum_{j\in\mathcal{K},(j\neq i)} \sigma^2_{a_{ij}} p_j^2 p_i^{-2} t^2 + \sigma^2_{b_i} p_i^{-2} t^2} \right\} \leq 1, \\
& \forall i \in \mathcal{K}, s \in \mathcal{S} \\
& \prod_{i\in\mathcal{K}} y_i \geq (1-\alpha) \\
& 0 \leq y_i \leq 1, \quad \forall i \in \mathcal{K} \\
& P_{min} \leq p_i \leq P_{max}, \quad \forall i \in \mathcal{K}
\end{aligned}
\tag{32}
$$

and

$$
\begin{aligned}
(JM_2)^{Ub}: \quad & \max_{\{(p,t,y)\in\mathbb{R}^{3K}_{++}\}} \prod_{i\in\mathcal{K}} t_i \\
\text{s.t.} \quad & \prod_{l\in\mathcal{K}} p_l^{-\delta_{il}} \left(\sum_{j\in\mathcal{K},(j\neq i)} \bar{c}_{ij} p_j t_i + \bar{d}_i t_i \right) \\
& + \left(e^{\frac{f_s}{2}} y_i^{\frac{g_s}{2}} \right) \left\{ \sqrt{\prod_{l\in\mathcal{K}} p_l^{-2\delta_{il}} \left(\sum_{j\in\mathcal{K},(j\neq i)} \sigma^2_{c_{ij}} p_j^2 t_i^2 + \sigma^2_{d_i} t_i^2 \right)} \right\} \leq 1, \\
& \forall i \in \mathcal{K}, s \in \mathcal{S} \\
& \prod_{i\in\mathcal{K}} y_i \geq (1-\alpha) \\
& 0 \leq y_i \leq 1, \quad \forall i \in \mathcal{K} \\
& P_{min} \leq p_i \leq P_{max}, \quad \forall i \in \mathcal{K}
\end{aligned}
\tag{33}
$$

respectively where the set $\mathcal{S} = \{1,\ldots,S\}$ corresponds to an index set associated with a set of linear functions. Notice that to obtain a convex reformulation of the constraints (16), one can use the standard variable transformations $x_i = \log(y_i)$, $r_i = \log(t_i)$ and $h_i = \log(p_i)$ for each $i \in \mathcal{K}$. Thus, the constraints (16) can be equivalently written as

$$
\begin{aligned}
& \sum_{j\in\mathcal{K},(j\neq i)} e^{h_j - h_i + r + \log(\bar{a}_{ij})} + e^{-h_i + r + \log(\bar{b}_i)} \\
& + \sqrt{e^{2\log(\phi^{-1}(e^{x_i}))} \left(\sum_{j\in\mathcal{K},(j\neq i)} e^{2h_j - 2h_i + 2r + \log(\sigma^2_{a_{ij}})} + e^{-2h_i + 2r + \log(\sigma^2_{b_i})} \right)} \leq 1, \\
& \forall i \in \mathcal{K}
\end{aligned}
\tag{34}
$$

Notice that we can replace the terms $\left(e^{\frac{f_s}{2}}y_i^{\frac{g_s}{2}}\right)$ for all $s \in \mathcal{S}$, $i \in \mathcal{K}$ in $(JM_1)^{Lb}$ and $(JM_2)^{Ub}$ by tangent linear functions. However, this can be performed once the log transformations have already been applied to convexify the problem [8]. This leads to the constraints (34). Thus, we approximate the function $2\log(\phi^{-1}(e^{x_i})) \geq F_s(x_i) = f_s x_i + g_s$ for all $s \in \mathcal{S}, i \in \mathcal{K}$. For this purpose, one can choose tangent lines of $2\log(\phi^{-1}(e^{x_i}))$ at different points in $[\log(1-\alpha), 0)$, say $\chi_1, \ldots, \chi_S$. Then, for each $s \in \mathcal{S}$, we have that

$$g_s = \frac{2e^{\chi_s}(\phi^{-1})^{(1)}(e^{\chi_s})}{\phi^{-1}(e^{\chi_s})}$$

and

$$f_s = -g_s\chi_s + 2\log(\phi^{-1}(e^{\chi_s}))$$

This is possible to achieve since the function $2\log(\phi^{-1}(e^{x_i}))$ is convex at the required interval. Consequently, we have that the feasible sets of (JM_1) and (JM_2) are contained in the feasible sets of $(JM_1)^{Lb}$ and $(JM_2)^{Ub}$, respectively. Finally, by reversing the log transformations, one can easily verify that $\phi^{-1}(y_i) \geq e^{\frac{f_s}{2}}y_i^{\frac{g_s}{2}}$ for all $s \in \mathcal{S}$, and $i \in \mathcal{K}$.

4.2 Sequential approximation methods

Now we explain the sequential approximation method used to compute upper and lower bounds for (JM_1) and (JM_2), respectively [11]. For the sake of brevity, we only explain the method when applied to (JM_1). The idea is simple and consists of fixing the variable $y = y^n$ at iteration n while satisfying the feasibility of the constraints (17)-(18). This allows solving the GP problem

$$\begin{aligned}
(JM_1)(y^n): \min_{\{(p,t)\in\mathbb{R}^{K+1}_{++}\}} \; & t^{-1} \\
\text{s.t.} \; & \sum_{j\in\mathcal{K},(j\neq i)} \bar{a}_{ij}p_j p_i^{-1}t + \bar{b}_i p_i^{-1}t \\
& + \phi^{-1}(y_i^n)\left\{\sqrt{\sum_{j\in\mathcal{K},(j\neq i)} \sigma^2_{a_{ij}}p_j^2 p_i^{-2}t^2 + \sigma^2_{\bar{b}_i}p_i^{-2}t^2}\right\} \\
& \leq 1, \quad \forall i \in \mathcal{K} \\
& P_{min} \leq p_i \leq P_{max}, \quad \forall i \in \mathcal{K}
\end{aligned}$$

Let $(p^n, t^n, \theta^n, v_n)$ denote an optimal solution of $(JM_1)(y^n)$, an optimal solution of the Lagrangian dual variable θ and the optimal objective function value, respectively [11]. We then compute the search direction parameters

$$\varphi_i = \theta_i^n(\phi^{-1})'(y_i^n) \sqrt{\sum_{j\in\mathcal{K},(j\neq i)} \sigma^2_{a_{ij}}\left(p_j^n\right)^2(p_i^n)^{-2}(t^n)^2 + \sigma^2_{b_i}(p_i^n)^{-2}(t^n)^2}$$

for each $i \in \mathcal{K}$ and update the y variable by solving the following GP problem

$$\begin{aligned}
(JM_1)(p^n, t^n): \min_{\{y\in\mathbb{R}^K_+\}} \; & \sum_{i\in\mathcal{K}} \varphi_i y_i \\
\text{s.t.} \; & y_i \leq \phi\left(\frac{1 - \sum_{j\in\mathcal{K},(j\neq i)} \bar{a}_{ij}p_j^n(p_i^n)^{-1}t^n - \bar{b}_i(p_i^n)^{-1}t^n}{\sqrt{\sum_{j\in\mathcal{K},(j\neq i)} \sigma^2_{a_{ij}}\left(p_j^n\right)^2(p_i^n)^{-2}(t^n)^2 + \sigma^2_{b_i}(p_i^n)^{-2}(t^n)^2}}\right), \forall i \in \mathcal{K} \\
& \prod_{i\in\mathcal{K}} y_i \geq (1-\alpha) \\
& 0 \leq y_i \leq 1, \forall i \in \mathcal{K}
\end{aligned}$$

where $\phi(\cdot)$ denotes the normal cumulative distribution function. The iterative sequential method is depicted in Algorithm 1

Algorithm 1 Sequential convex approximation method

Require: An instance of problem (JM_1)
Ensure: An upper bound for (JM_1)
1: **Initialization step:**
2: Choose an initial point y^0 of y satisfying the constraints (17)-(18).
3: Solve $(JM_1)(y^0)$ and use the optimal solution obtained for solving $(JM_1)(p^0, t^0)$.
4: Set $n = 1$. Denote by y^n the optimal solution of $(JM_1)(p^0, t^0)$
5: **Iterative step:**
6: **while** $(\|y^{n-1} - y^n\| > \varepsilon$ and number of iterations $<= MaxIter)$ **do**
7: Solve $(JM_1)(y^n)$ and use the optimal solution obtained for solving $(JM_1)(p^n, t^n)$.
8: Let $\bar{y}$ denote the optimal solution of $(JM_1)(p^n, t^n)$
9: $y^{n+1} = y^n + \tau(\bar{y} - y^n)$. Here, $\tau \in (0, 1)$ is the step length.
10: Set $n = n + 1$.
11: **end while**
12: **return** the best solution found (p^n, t^n, y^n)

Finally, we present a single condensed sequential approximation method used to compute lower bounds for $Q(\delta, \beta)$ according to [24]. This procedure is depicted in Algorithm 2 as follows. The procedure is simple and starts by initializing the input parameter values δ and β while ensuring that the conditions (29) are satisfied. Then, we iterative until the difference between the objective function values obtained with model $Q(\delta, \beta)$ in two consecutive iterations is less than or equal to a small positive value ϵ. Notice that at each iteration, the input parameters δ and β are updated according to the monomials approximations (25). Finally, the best solution obtained for $Q^* = Q(\delta^*, \beta^*)$ is returned by the algorithm together with the optimal values of parameters δ^* and β^*. Recall that to solve models (IM_2) and (JM_2), we use these parameter values. Notice that Algorithm 2 can be sensitive to the initial values of δ and β. Consequently, to increase the chances of obtaining a global optimal solution for $Q = Q(\delta, \beta)$, an intuitive approach is to run Algorithm 2 several times by using different initial values for the parameter δ and β. Although this approach does not guarantee finding the global optimal solution to the problem, we can still measure the difference between the stochastic and deterministic models derived from $Q(\delta^*, \beta^*)$.

5 Numerical experiments

In this section, we conduct substantial numerical experiments to compare all the proposed models and the sequential approximation algorithms. For this purpose, we implement python codes using CVXPY version 1.1.12 interfaced with Mosek solver version 9.2.42 [40–42]. The numerical experiments were carried out on an Intel(R) 64 bits core (TM) with 2.50 GHz and 12GB of RAM under Windows 10. We present numerical results for all the proposed models derived for (M_1) and (M_2) where the objectives are to maximize the worst user signal-to-interference noise ratio and the total capacity of the network, respectively. In particular, for (M_1), we consider instances dimensions ranging from $K = 10$ to $K = 50$ users. Whereas for (M_2), we generate instances ranging from $K = 10$ to $K = 22$ users. We notice that the objective functions of both models (M_1) and (M_2) deteriorate significantly when the number of users increases. This is clear since the more users the network has, the higher the interference generated. In particular, for (M_2) we did not generate instances with more than $K = 22$ users because doing this leads to infeasible solutions. We arbitrarily set the input parameters values to $P_{min} = 0.1$, $P_{max} = 0.5$ and generate

Algorithm 2 Single condensed sequential approximation method

Require: An instance of problem $Q(\delta, \beta)$
Ensure: A lower bound for $Q(\delta, \beta)$
Initialization step:
Randomly generate positive values for the parameters δ and β satisfying the conditions (29).
Solve the GP problem $Q(\delta, \beta)$.
Let $(p, t) \in \mathbb{R}^{2K}$ and V_Q denote the optimal solution and objective function value obtained.
Iterative step:
while (True) **do**
  for $i \in \mathcal{K}$ **do**
    $\beta_i = \frac{b_i}{\sum_{l \in \mathcal{K}} a_{il}\hat{p}_l + b_i}$
    for $j \in \mathcal{K}$ **do**
      $\delta_{ij} = \frac{a_{ij}\hat{p}_j}{\sum_{l \in \mathcal{K}} a_{il}\hat{p}_l + b_i}$
    end for
  end for
  Solve the GP problem $Q(\delta, \beta)$.
  Let $(p, t) \in \mathbb{R}^{2K}$ and W_Q denote the optimal solution and objective function value obtained.
  if ($| W_Q - V_Q | \leq \epsilon$ or number of $Iterations \geq MaxIt$) **then**
    Break
  else
    $W_Q = V_Q$
  end if
end while
return best solution obtained $(p^*, t^*, W_Q^*, \delta^*, \beta^*)$

the complex vectors $g_i \in \mathbf{C}^{T\times 1}$, and $g_i^H \in \mathbf{C}^{1\times T}$ for each $i \in \mathcal{K}$ according to an independent complex Gaussian distribution function with zero mean and variance equal to one. Then, we multiply each of these vectors by a factor of 2.5. Finally, the parameter σ_i for each $i \in \mathcal{K}$ is also generated according to an independent complex Gaussian distribution function with zero mean and variance equal to one. The parameters a_{ij} and b_i are calculated as explained in Sect. 3. Without loss of generality, we assume in our stochastic GP models that $\bar{a}_{ij} = a_{ij}$ and $\bar{b}_i = b_i$ for all $i,j \in \mathcal{K}$ coincide with the means of the random variables. In all our experiments, we vary the parameter values of $\alpha \in \{0.1; 0.25\}$, and $\sigma_{b_i}, \sigma_{a_{ij}} \in \{10^{-3}; 10^{-2}; 10^{-1}; 1; 2\}$ for all $i,j \in \mathcal{K}$. In order to solve the GP models $(JM_1)^{Lb}$ and $(JM_2)^{Ub}$, we consider the set $\mathcal{S} = \{5, 10, 20\}$ to reference the number of tangent linear segments. Finally, the parameter values in Algorithms 1 and 2 are set to $\varepsilon = 10^{-4}$, $MaxIter = 50$, $\tau = 0.5$, $y_i = 0.9999999$ for all $i \in \mathcal{K}$ as initial values, and $\epsilon = 10^{-6}$, $MaxIt = 1000$, respectively. Notice that the initial values of y_i for all $i \in \mathcal{K}$ give a value of 5.199337582290661 for the inverse of the standard normal cumulative distribution function. Thus, avoiding the value of 1 which gives infinite for this function. Moreover, these values satisfy all the required constraints of the GP models of Algorithm 1.

5.1 Worst user SINR

In Table 1 of Annex A of the supplementary material, we present average numerical results for the GP models (M_1), (IM_1), and (JM_1) over 20 samples. More precisely, in column 1 we present the number of users of each particular instance. Whilst in columns 2–5, 6–9 and 10–13 we present the optimal objective function value, the CPU time in seconds required by Mosek and CVXPY solvers and the standard deviation obtained with the models (M_1), (IM_1) and (JM_1), respectively. In particular, model (JM_1) is solved with Algorithm 1. Consequently, in column 14, we present the number of iterations required by Algorithm 1 to obtain the solution.

From Table 1, first, we observe that the optimal objective function values obtained with model (JM_1) are larger than those reported for (IM_1). In turn, the objective values obtained with (IM_1) are larger than the ones obtained with (M_1). Next, we see that these differences increase when using higher values of σ and α. Notice that by using higher values for the parameters σ and α, we can obtain more conservative solutions to the problem. Next, we observe that the CPU time required by Mosek solver is significantly smaller than the one reported for CVXPY. This can be explained by the parser property of CVXPY solver which is required to convexify the GP problem [8]. Next, we observe that the standard deviation values are large and nearly the same for all the instances. This fact gives an idea of how sensitive the solutions obtained with the GP models are depending on the input data. Finally, we observe that the number of iterations is on average less than 22 which evidences the effectiveness achieved by the Algorithm 1.

In Tables 2, 3, 4, and 5 (See Annex A), we report numerical results obtained with model (JM_1) using randomly generated instances for different values of α and σ. We solve the same instances in these tables. The main purpose of these tables is to show how tight the GP models using tangent piece-wise linear functions are when compared to the sequential approximation Algorithm 1. The legend of these tables is the same and is as follows. In column 1, we present the number of users considered in the network. Next, in columns 2–6 we present the number of tangent linear segments used in model $(JM_1)^{Lb}$ and its number of constraints, its optimal objective function value, and the CPU times in seconds obtained with Mosek and CVXPY solvers, respectively. From columns 7 to 10, we present the optimal objective function value of (JM_1) obtained with Algorithm 1, the CPU times in seconds required by Mosek and CVXPY solvers, and the number of iterations required by Algorithm 1 to solve (JM_1). Finally, in column 11 we respectively report the gaps that we compute by $\left[\frac{v((JM_1))-v((JM_1)^{Lb})}{v((JM_1))}\right] * 100$ where $v(\cdot)$ denotes the optimal objective function value of the respective model. Notice that we report these gap values for a different number of tangent linear segments used in model $(JM_1)^{Lb}$. From Tables 2, 3, 4, and 5, we mainly observe that the objective function values obtained with (JM_1) are slightly higher than those obtained with $(JM_1)^{Lb}$. In particular, we see that the gap values reported in column 11 in each of these tables become smaller when using more tangent linear functions in $(JM_1)^{Lb}$. Similarly, we observe that the gap values obtained with $\sigma = 0.01$ are smaller than those obtained when using $\sigma = 0.1$. Next, we also see that the optimal objective function values reported in Tables 4 and 5 for both models $(JM_1)^{Lb}$ and (JM_1) are larger than in Tables 2 and 3, respectively. We notice that this is a consequence of using a larger value of parameter α which is equivalent to imposing a stronger probabilistic constraint in each model. As a consequence, we obtain more conservative solutions with each model.

Another relevant observation is that the CPU times reported in columns 5 and 6, and in columns 8 and 9 for all the instances in each of these tables are significantly higher for CVXPY than for the Mosek solver. Recall that the CPU time of CVXPY includes the CPU time of the Mosek solver. This shows that CVXPY spends a considerable amount of time transforming the problem from GP format

to a convex problem that is solvable by the Mosek solver. Finally, we observe that the number of iterations required by Algorithm 1 to solve all the instances remains nearly the same in Tables 2, 3, 4, and 5.

To give more insights regarding the conservatism level achieved with the solutions obtained with models (M_1), (IM_1), (JM_1) and $(JM_1)^{Lb}$, we report in Figs. 1-4 the number of violated constraints and amount of constraint violations for an instance with $K = 30$ users while using parameter values of $\alpha = 0.25$ and $\sigma = \{0.1, 1\}$. More precisely, we save the optimal solutions obtained with the models (M_1), (IM_1), (JM_1), and $(JM_1)^{Lb}$ for a particular instance randomly generated. And then, we randomly generate another 100 instances (scenarios) and count the number of violated constraints in (8) and their violated amounts obtained by replacing the saved solutions.

From Figs. 1 and 2, we mainly observe that the optimal saved solution obtained with (IM_1) is more robust than the one obtained with (M_1) in the sense that it allows obtaining less violated constraints and a lower amount of violation. Similarly, we observe that the optimal saved solution obtained with (JM_1) using Algorithm 1 is more conservative than the one obtained with (IM_1). Finally, we see that the solution obtained with $(JM_1)^{Lb}$ is less conservative than the one obtained with (JM_1) using Algorithm 1. In conclusion, we see that the solution obtained with the joint chance-constrained model (JM_1) is significantly more robust than the ones obtained with the other models. In Figs. 3 and 4, we observe similar trends as in Figs. 1 and 2. Ultimately, we notice that the higher the value of parameter σ, the higher the level of robustness achieved with the obtained solutions.

5.2 Maximum capacity

Now, we report numerical results for the second power allocation problem which is aimed to maximize the total capacity of the wireless network. In particular, in Table 6 (See annex B in the supplementary material), we report numerical results for $Q(\delta, \beta)$. These results are obtained with the condensed sequential approximation Algorithm 2. In this table, we do also report numerical results for the model (IM_2). Recall that the latter model is solved using the best values obtained for the parameters δ and β when solving $Q(\delta, \beta)$ with Algorithm 2. In Table 6, column 1 shows the number of users of each instance. Columns 2 to 6 present the objective function value of $Q(\delta, \beta)$, the capacity achieved which is computed by taking the logarithm of the objective function value, the CPU time in seconds required by the Mosek and CVXPY solvers to obtain the solutions and the number of iterations required by Algorithm 2. Columns 7–10 report the optimal objective function value of model (IM_2), its capacity which is again computed by taking the logarithm of the objective value, and the CPU times in seconds required by the Mosek and CVXPY solvers, respectively. The instances are randomly generated and solved for different input values for the parameters α and σ. From Table 6, first, we observe that the capacity values decrease significantly when the number of users increases. This is evident since the higher the number of users, the higher the interference in the network. Next, we also see that the CPU times required by CVXPY increase considerably with the number of users. Similarly, the number of iterations required by Algorithm 2 to converge also increases with the number of users. Next, we observe that the optimal objective function values obtained with (IM_2) decrease when the parameter σ increases. On the opposite, these objective values increase with an increase of parameter α. Finally, we observe that the CPU time values required by CVXPY are significantly higher than those required by the Mosek solver.

In Tables 7 and 8 in annex B, we present upper bounds obtained with model $(JM_2)^{Ub}$ and lower bounds obtained with model (JM_2) while using the sequential approximation Algorithm 1 for given and fixed values of δ and β. The values of δ and β are obtained by solving $Q(\delta, \beta)$ with Algorithm 2 for the instances in Table 6 of annex B. In Tables 6, 7, and 8, we solve the same instances. In Tables 7 and 8, the legends are the same. In column 1, we present the number of users of each instance. Next, in columns 2 and 3, we present the number of tangent linear segments and constraints of model $(JM_2)^{Ub}$. Subsequently, in columns 4, 5, and 6, we report the optimal objective function values of $(JM_2)^{Ub}$ and the CPU times in seconds required by the Mosek and CVXPY solvers, respectively. Similarly, in columns 7–10 we present the optimal objective function values of model (JM_2), the CPU times in seconds required by the Mosek and CVXPY solvers, and the number of

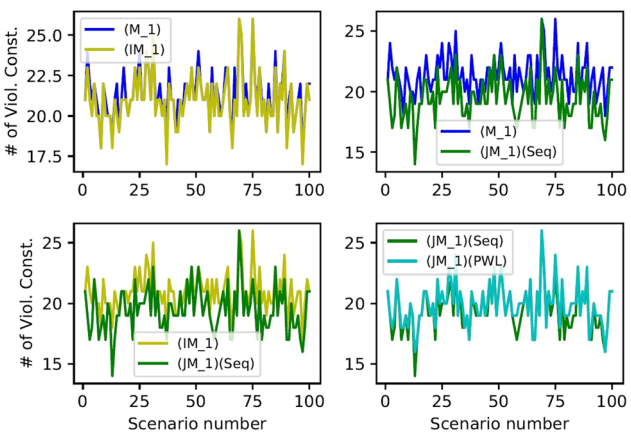

Fig. 1 Number of violated constraints for each randomly generated instance using $K = 30$, $\alpha = 0.25$ and $\sigma = 0.1$

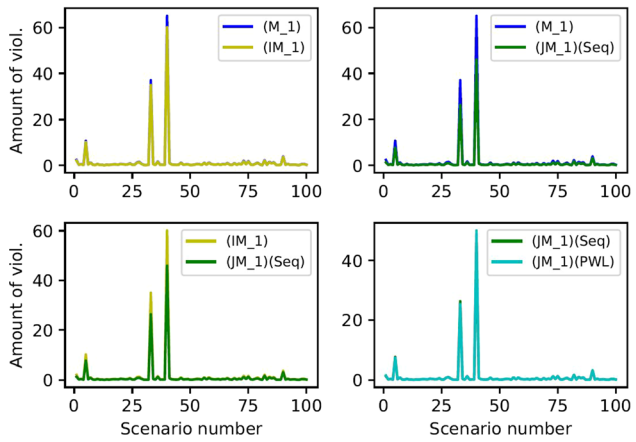

Fig. 2 The total amount of constraint violation for each randomly generated instance using $K = 30$, $\alpha = 0.25$ and $\sigma = 0.1$

iterations obtained when solving (JM_2) with Algorithm 1, respectively. Finally, in column 11 we present gap values which are computed by $\left[\frac{v\left((JM_2)^{Ub}\right)-v((JM_2))}{v((JM_2))}\right] * 100$ where $v(\cdot)$ denotes the optimal objective function value of the respective model. From Tables 7 and 8, we mainly observe that the optimal objective function values obtained with $(JM_2)^{Ub}$ and (JM_2) get closer when using a higher number of piece-wise linear segments ($S = 20$). We further notice that these objective values deteriorate when using lower and higher values of α and σ, respectively. Next, we see that the objective function values decrease when more users are present in the network. Notice that we do not consider more than 22 users. Otherwise, we may obtain infeasible solutions with negative capacity values. We also observe that the CPU time values obtained with Algorithm 1 are larger than those obtained with $(JM_2)^{Ub}$ for all the tested instances using less than $S = 20$ linear segments. For the remaining ones, we observe the opposite situation.

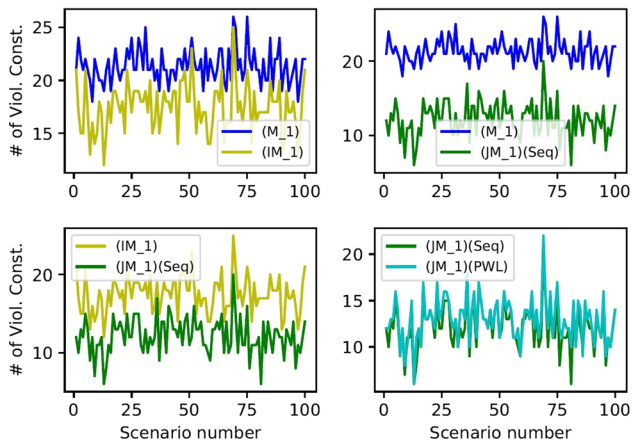

Fig. 3 Number of violated constraints for each randomly generated instance using $K = 30$, $\alpha = 0.25$ and $\sigma = 1$

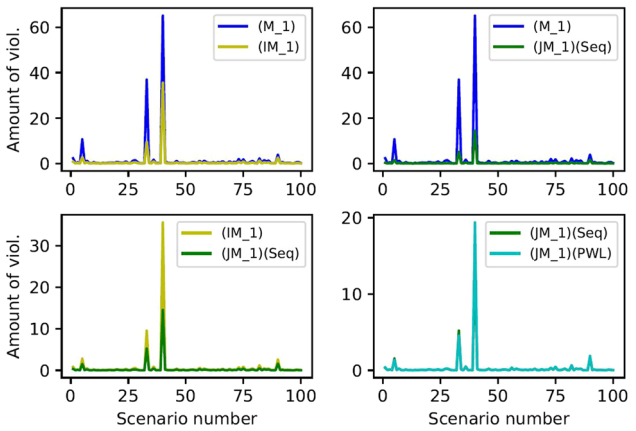

Fig. 4 The total amount of constraint violation for each randomly generated instance using $K = 30$, $\alpha = 0.25$ and $\sigma = 1$

Finally, we see that the number of iterations required by Algorithm 1 to solve all the instances is very stable. To give more insights concerning the solutions obtained with the condensed sequential approximation Algorithm 2, we plot in Figs. 5 and 6, the optimal solutions and the number of iterations obtained with $Q(\delta, \beta)$ for $K = 10$ and $K = 14$ users while generating different initial input values for the parameters δ and β. The idea is to provide some empirical evidence indicating that the solutions obtained with Algorithm 2 are near the global optimal ones. In particular, in Figs. 5 and 6 we randomly generate 100 and 20 initial sample values for the parameters δ and β, respectively. All these values are generated while satisfying the conditions imposed in problem (28)-(29). In Fig. 6, we only generate 20 samples for δ and β since the CPU times required to solve $Q(\delta, \beta)$ with Algorithm 2 become larger for $K = 14$ users. From Figs. 5 and 6, we see that it is not always possible to obtain the same optimal solution when using different initial samples for the parameters δ and β. This confirms that Algorithm 2 does not guarantee finding the global optimal solution to the problem. It only allows finding locally optimal solutions to the problem. However, we also notice that a recurrent maximum value is attained for many samples which might suggest that it is indeed the global optimal solution. Regarding the number of iterations, we do not observe a clear pattern as these values oscillate within a large range of possible values.

Finally, to report some empirical evidence that we observed when solving our instances regarding the slow convergence of Algorithm 2, in Fig. 7 we plot 10 curves with the optimal solutions obtained in each iteration during 10 runs of Algorithm 2 while using different initial values for the parameters δ and β. From Fig. 7, we mainly observe that only after 100 iterations do we start finding better objective function values for the problem. Also, we notice that only for 3 out of 10 runs do we obtain the larger

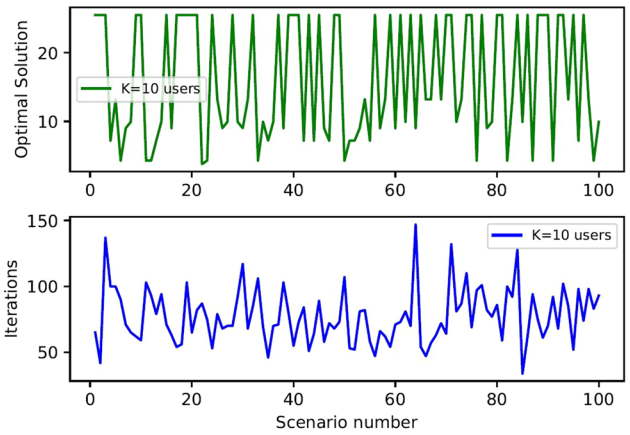

Fig. 5 Optimal solutions and the number of iterations obtained with Algorithm 2 for 100 initial samples of parameters δ and β using $K = 10$

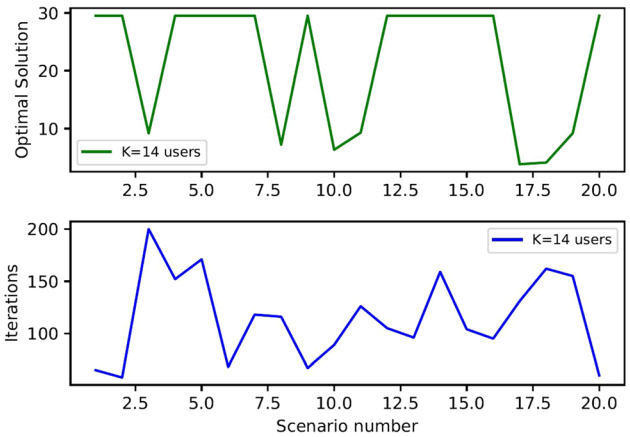

Fig. 6 Optimal solutions and the number of iterations obtained with Algorithm 2 for 20 initial samples of parameters δ and β using $K = 14$

objective function values which are above the value of 10. Most of the remaining runs converge in less than 250 iterations and with a lower objective function value. This explains the CPU time values reported in Table 6 for Algorithm 2. To conclude, we cannot ensure that global optimal solutions are obtained with Algorithm 2. However, for a few small-size instances, we provide some empirical evidence indicating that the solutions obtained are near-optimal ones.

6 Conclusions

In this paper, we consider the problem of power allocation for 5 G wireless networks using massive multiple input multiple output technologies. We propose two non-linear optimization models where the aims are to maximize the worst user signal-to-interference noise ratio and the total

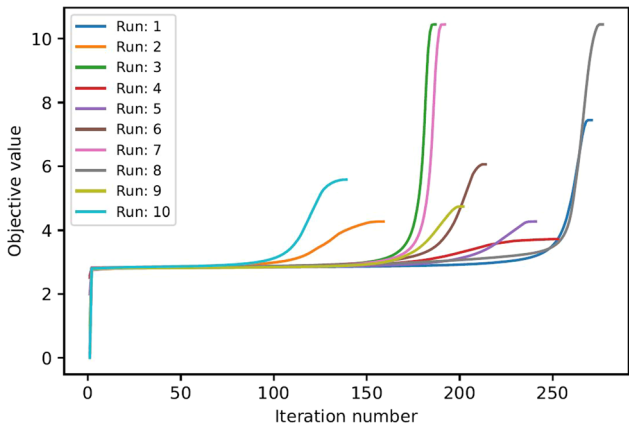

Fig. 7 Slow convergence of the condensed sequential approximation method reporting optimal solutions and the number of iterations obtained for an instance of $K = 16$ users while using different initial values of parameters δ and β

capacity of the network subject to power constraints. In particular, our first model is transformed into an equivalent geometric programming problem. Whereas the second one is formulated as an equivalent signomial programming problem. Since the latter problem is non-convex, we propose an approximated geometric model to compute lower bounds. This is achieved by using the arithmetic–geometric mean inequality. Subsequently, we derive stochastic formulations for each geometric programming model to deal with the uncertainty of wireless channels. More precisely, we include individual and joint probabilistic constraints on each GP model. Finally, we compute lower and upper bounds by using sequential convex and piece-wise linear methods. Substantial numerical experiments are conducted to compare all the proposed models and algorithms. Our numerical experiments indicate the following relevant conclusions.

1. First, we conclude that the use of joint chance constraints allows obtaining more conservative solutions for the power allocation problems than using individual chance constraints or using directly the deterministic models.
2. Next, we observe that the sequential approximation Algorithm 1 together with the piece-wise GP models allows obtaining tight bounds while using joint chance constraints. The latter is a crucial fact as it shows that we can approximate the globally optimal solutions to the problems in an efficient manner. Moreover, we observe that this sequential method requires only a few iterations to converge for most of the tested instances.
3. For the signomial problem, we mainly observe that the condensed sequential approximation method requires a significantly larger number of iterations to converge than the other sequential method. Although, as shown

in the numerical results section, we can still use it with different initial values for the required parameters to improve the solutions obtained with the deterministic model.

4. We observe that independently of the parameter values obtained when solving the deterministic signomial problem, we can still obtain tight bounds for the stochastic models derived from it.
5. Finally, as part of future research, we remark that all the modeling approaches and solution methods studied in this paper can be further investigated and applied to many other relevant problems related to resource allocation in wireless networks. Ultimately, we believe that novel algorithmic approaches including meta-heuristics should also be part of future research, especially for solving the signomial and stochastic programming models.

Supplementary Information The online version contains supplementary material available at https://doi.org/10.1007/s11276-023-03295-8.

Acknowledgements The authors acknowledge the financial support from Project: FONDECYT No. 11180107 and from Project Dicyt 062313AS.

Data availability The datasets generated during and/or analyzed during the current study are available from the corresponding author on reasonable request.

Declarations

Conflict of interest The authors have no conficts of interest to declare that are relevant to the content of this article.

References

1. Chiasserini, C., & Magnan, A. IEEE 5G for the Automotive Domain, https://futurenetworks.ieee.org/images/files/pdf/applications/5G-for-the-Automotive-Domain030518.pdf
2. Somisetty, M. Big Data Analytics in 5G, https://futurenetworks.ieee.org/images/files/pdf/applications/Data-Analytics-in-5G-Applications030518.pdf
3. Markakis, E., & Politis, I., 5G Emergency Communications, https://futurenetworks.ieee.org/images/files/pdf/applications/Emergency-Communications030518.pdf
4. Orsino, A., Yilmaz, O. N.C., & Torsner, J. Ericsson Research, Factories of the Future Enabled by 5G Technology, https://futurenetworks.ieee.org/images/files/pdf/applications/Factories-of-the-Future-Enabled-by-5G-Technology_030518.pdf
5. Rao, K. The Path to 5G for Health Care, https://futurenetworks.ieee.org/images/files/pdf/applications/5G–Health-Care030518.pdf
6. Mangra, N., & Ghasempour, A. Smart Cities: Connected Ecosystem of Ecosystems, https://futurenetworks.ieee.org/images/files/pdf/applications/Smart-Cities_030518.pdf
7. IEEE 5G and Beyond Technology Roadmap, https://futurenetworks.ieee.org/images/files/pdf/ieee-5g-roadmap-white-paper.pdf
8. Boyd, S., Kim, S. J., Vandenberghe, L., & Hassibi, A. (2007). A tutorial on geometric programming. *Optimization and Engineering, 8*(67), 67–127.
9. Duffin, R., Peterson, E., & Zener, C. (1967). *Geometric programming-theory and application*. New York: Wiley.
10. Parsaeefard, S., Jumba, V., Shoaei, A. D., Derakhshani, M., & Le-Ngoc, T. (2021). User association in cloud RANs with massive MIMO. *IEEE Transactions on Cloud Computing, 9*(2), 821–833.
11. Liu, J., Lisser, A., & Chen, Z. (2016). Stochastic geometric optimization with joint probabilistic constraints. *Operations Research Letters, 44*, 687–691.
12. Azizi, A., Parsaeefard, S., Javan, M. R., Mokari, N., & Yanikomeroglu, H. (2020). Profit maximization in 5G+ networks with heterogeneous aerial and ground base stations. *IEEE Transactions on Mobile Computing, 19*(10), 2445–2460.
13. Bashar, M., Cumanan, K., Burr, A. G., Ngo, H. Q., Larsson, E. G., & Xiao, P. (2019). Energy efficiency of the cell-free massive mimo uplink with optimal uniform quantization. *IEEE Transactions on Green Communications and Networking, 3*(4), 971–987.
14. Amani, N., Pedram, H., Taheri, H., & Parsaeefard, S. (2019). Energy-efficient resource allocation in heterogeneous cloud radio access networks via BBU offloading. *IEEE Transactions on Vehicular Technology, 68*(2), 1365–1377.
15. Tweed, D., Derakhshani, M., Parsaeefard, S., & Le-Ngoc, T. (2017). Outage-constrained resource allocation in uplink NOMA for critical applications. *IEEE Access, 5*, 27636–27648.
16. Parsaeefard, S., Dawadi, R., Derakhshani, M., Le-Ngoc, T., & Baghani, M. (2017). Dynamic resource allocation for virtualized wireless networks in massive-MIMO-Aided and Fronthaul-limited C-RAN. *IEEE Transactions on Vehicular Technology, 66*(10), 9512–9520.
17. Lakani, S., & Gagnon, F. (2017). Optimal design and energy efficient binary resource allocation of interference-limited cellular relay-aided systems with consideration of queue stability. *IEEE Access, 5*, 8459–8474.
18. Gao, H., Su, Y., Zhang, S., & Diao, M. (2019). Antenna selection and power allocation design for 5G massive MIMO uplink networks. *China Communications, 16*(4), 1–15.
19. Benmimoune, M., Driouch, E., Ajib, W., & Massicotte, D. (2015). Joint Transmit Antenna Selection and User Scheduling for Massive MIMO Systems, in IEEE Wireless Communications and Networking Conference (WCNC). https://ieeexplore.ieee.org/document/7127500
20. Pedram, M., & Wang, L. (2020). Energy efficiency in 5G cellular network systems. *IEEE Design and Test, 37*(1), 64–78.
21. Zhang, J., Zhang, Y., Xiang, L., Sun, Y., Kwan Ng, D. W., & Jo, M. (2021). Robust energy-efficient transmission for wireless-powered d2d communication networks. *IEEE Transactions on Vehicular Technology, 70*(8), 7951–7965.
22. Le, A. T., Ha, N. D. X., Do, D. T., Silva, A., & Yadav, S. (2021). Enabling user grouping and fixed power allocation scheme for reconfigurable intelligent surfaces-aided wireless systems. *IEEE Access, 9*, 92263–92275.
23. Lu, H., Jiang, X., & Chen, C. W. (2021). Distortion-aware cross-layer power allocation for video transmission over multi-user NOMA systems. *IEEE Transactions on Wireless Communications, 20*(2), 1076–1092.
24. Chiang, M., Tan, C. W., Palomar, D. P., Ońeill, D., & Julian, D. (2007). Power control by geometric programming. *IEEE Transactions on Wireless Communications, 6*(7), 2640–2651.
25. Cheng, J., Delage, E., & Lisser, A. (2014). Distributionally robust stochastic knapsack problem. *SIAM Journal on Optimization, 24*(3), 1485–1506.

26. Cheng, J., & Lisser, A. (2012). A second-order cone programming approach for linear programs with joint probabilistic constraints. *Operations Research Letters, 40*, 325–328.
27. Lobo, M., Vandenberghe, L., Boyd, S., & Lebret, H. (1998). Applications of second-order cone programming. *Linear Algebra and its Applications, 284*, 193–228.
28. Luedtke, J., Ahmed, S., & Nemhauser, G. (2010). An integer programming approach for linear programs with probabilistic constraints. *Mathematical Programming, 122*, 247–272.
29. Prékopa, A. (1995). Stochastic Programming, in: Mathematics and Its Applications, 324, Springer Netherlands.
30. Prékopa, A. (1970). On probabilistic constrained programming Proceedings of the Princeton Symposium on Mathematical Programming. Princeton University Press, Princeton.
31. Shapiro, A., Dentcheva, D., & Ruszczynski, A. (2009). Lectures on stochastic programming: Modeling and theory, 436. SIAM Philadelphia, Series on Optimization, 9 of MPS/SIAM, Philadelphia.
32. Adasme, P., & Lisser, A. (2014). Stochastic and semidefinite optimization for scheduling in orthogonal frequency division multiple access networks. *Journal of Scheduling, 17*(5), 445–469.
33. Adasme, P., & Lisser, A. (2016). Uplink scheduling for joint wireless orthogonal frequency and time division multiple access networks. *Journal of Scheduling, 19*(3), 349–366.
34. Dupacová, J. Stochastic geometric programming: approaches and applications, In V. Brozová, R. Kvasnicka, eds., Proceedings of MME09, 2009, pp. 63-66.
35. Rao, S. S. (1996). *Engineering Optimization: Theory and Practice* (3rd ed.). New York: Wiley- Interscience.
36. Liu, J., Peng, S., Lisser, A., & Chen, Z. (2020). Rectangular chance constrained geometric optimization. *Optimization and engineering, 21*, 537–566.
37. Haleem, M. A. (2018). On the Capacity and Transmission Techniques of Massive MIMO Systems. *Wireless Communications and Mobile Computing*. https://doi.org/10.1155/2018/9363515
38. Adasme, P., Soto, I., Juan, E. S., Seguel, F., & Firoozabadi, A. D. (2020). Maximizing Signal to Interference Noise Ratio for Massive MIMO: A Mathematical Programming Approach, 2020 South American Colloquium on Visible Light Communications (SACVC), 1-6. https://ieeexplore.ieee.org/document/9129889
39. Valduga, S., Deneire, L., Pardo, R., Almeida, A., Maciel, T., & Mota, J. (2018). Low complexity heuristics to beam selection and rate adaptation in sparse massive MIMO systems. *Transactions on Emerging Telecommunication Technologies, 29*(9), e3459.
40. Diamond, S., & Boyd, S. (2016). CVXPY: A Python-embedded modeling language for convex optimization. *The Journal of Machine Learning Research, 17*(83), 1–5.
41. Agrawal, A., Verschueren, R., Diamond, S., & Boyd, S. (2018). A rewriting system for convex optimization problems. *Journal of Control and Decision, 5*(1), 42–60.
42. MOSEK solver version 9.2.42, 2021, https://www.mosek.com/. MOSEK is a software package for the solution of linear, mixed-integer linear, quadratic, mixed-integer quadratic, quadratically constraint, conic and convex nonlinear mathematical optimization problems.
43. Mohajer, A., Daliri, M. S., Mirzaei, A., Ziaeddini, A., Nabipour, M., & Bavaghar, M. (2022). Heterogeneous Computational Resource Allocation for NOMA: Toward Green Mobile Edge-Computing SystemsIEEE Transactions on Services Computing 1-14. https://doi.org/10.1109/TSC.2022.3186099
44. Mohajer, A., Bavaghar, M., & Farrokhi, H. (2020). Mobility-aware load Balancing for Reliable Self-Organization Networks: Multi-agent Deep Reinforcement Learning, Reliability Engineering & System Safety, Volume 202, https://doi.org/10.1016/j.ress.2020.107056
45. Mohajer, A., Sorouri, F., Mirzaei, A., Ziaeddini, A., Rad, K. J., & Bavaghar, M. (2022). Energy-Aware Hierarchical Resource Management and Backhaul Traffic Optimization in Heterogeneous Cellular Networks, in IEEE Systems Journal, 1-12. https://doi.org/10.1109/JSYST.2022.3154162

Pablo Adasme is an associate researcher and full professor in computer science at the Electrical Engineering Department of the Universidad de Santiago de Chile. He was born in 1972 in Santiago, Chile. He obtained the title of Industrial Engineer together with B. Sc. and M. Sc. degrees from Universidad de Santiago de Chile in 2000 and 2003, respectively. In 2010, he received a Ph.D. degree in computer science from the Université de Paris Sud 11, in Paris, France. Currently, his main research interests are related to deterministic and stochastic combinatorial optimization problems applied to a diverse range of engineering domains including wireless communications, signal processing, network design, and energy problems.

Abdel Lisser is a full Professor in Computer Science laboratory of University of Paris Sud since 2001. He was heading research group at France Telecom from Research Center 1996 to 2001 and research engineer at France Telecom Research Center from 1988 to 1996. He got the Ph.D. at the University of Paris Dauphine in Computer Science in 1987 and the Habilitation thesis at the University of Paris Nord in 2000. His main research area is combinatorial and stochastic optimization with application to telecommunication and recently energy problems.